

Extracting Modified Microtubules from Mammalian Cells to Study Microtubule-Protein Complexes by Cryo-Electron Microscopy

Jitske Bak¹, Lisa Landskron¹, Thijn R. Brummelkamp¹, Anastassis Perrakis¹

¹ Oncode Institute and Division of Biochemistry, Netherlands Cancer Institute

Corresponding Author

Anastassis Perrakis

a.perrakis@nki.nl

Citation

Bak, J., Landskron, L., Brummelkamp, T.R., Perrakis, A. Extracting Modified Microtubules from Mammalian Cells to Study Microtubule-Protein Complexes by Cryo-Electron Microscopy. *J. Vis. Exp.* (193), e65126, doi:10.3791/65126 (2023).

Date Published

March 3, 2023

DOI

10.3791/65126

URL

jove.com/video/65126

Abstract

Microtubules are an important part of the cytoskeleton and are involved in intracellular organization, cell division, and migration. Depending on the posttranslational modifications, microtubules can form complexes with various interacting proteins. These microtubule-protein complexes are often implicated in human diseases. Understanding the structure of such complexes is useful for elucidating their mechanisms of action and can be studied by cryo-electron microscopy (cryo-EM). To obtain such complexes for structural studies, it is important to extract microtubules containing or lacking specific posttranslational modifications. Here, we describe a simplified protocol to extract endogenous tubulin from genetically modified mammalian cells, involving microtubule polymerization, followed by sedimentation using ultracentrifugation. The extracted tubulin can then be used to prepare cryo-electron microscope grids with microtubules that are bound to a purified microtubule-binding protein of interest. As an example, we demonstrate the extraction of fully tyrosinated microtubules from cell lines engineered to lack the three known tubulin-detyrosinating enzymes. These microtubules are then used to make a protein complex with enzymatically inactive microtubule-associated tubulin detyrosinase on cryo-EM grids.

Introduction

Microtubules are a crucial part of the cytoskeleton; they are involved in different functions such as cell migration and division but also contribute to intracellular organization. To adapt to different functional fates, microtubules interact with a variety of microtubule-associated proteins (MAPs), enzymes, and other proteins, which we will collectively

refer to as "microtubule-interacting proteins." The microtubule binding of these proteins can be guided by different tubulin modifications, commonly referred to as the "tubulin code"¹. Examples of this preference are the mitotic centromere-associated kinesin (MCAK)² and the dynein-dynactin CAP-Gly domain of p150³, which preferably associate with

tyrosinated tubulin, while the kinesin motors centromere-associated protein E (CENP-E)⁴ and kinesin-2⁵ prefer tubulin that lacks the C-terminal tyrosine.

While a variety of methods can be employed to study microtubule-protein interactions, cryo-electron microscopy (cryo-EM) is often used to study these interactions at near-atomic resolution^{6,7}. In recent years, cryo-EM structures have revealed how large motor proteins such as dynein^{8,9,10} and kinesin¹¹, +TIP proteins such as EB3^{12,13} and MCAK¹⁴, other proteins such as Tau^{15,16}, and even small molecules such as paclitaxel, peloruside, and zampanolide¹⁷ interact with microtubules. To study microtubule-protein interactions, microtubules are typically extracted from the porcine brain¹⁸. Following this, most *in vitro* studies, including cryo-EM microtubule structures, are carried out using porcine brain tubulin. The results of these studies, therefore, obscure the importance of the heterogeneous nature of tubulin modifications¹⁹ between tissues and cell types. This creates a particular problem when investigating a protein that requires or prefers a specific modification to bind to microtubules. This can be illustrated with tyrosinated tubulin, the substrate for microtubule detyrosinase MATCAP.

Detyrosination is a tubulin modification in which the C-terminal amino acid tyrosine of α -tubulin is lacking, which is associated with mitotic, cardiac, and neuronal function²⁰. While fully tyrosinated microtubules are the ideal substrate for MATCAP, this is largely absent in commercially available microtubules from the porcine brain due to the function of the vasohibins^{21,22} and MATCAP²³ detyrosinases in this tissue^{22,23,24,25,26}. Although commercially available HeLa tubulin does mostly contain tyrosinated microtubules, detyrosination could occur, and this source of tubulin is,

therefore, less suitable for creating a uniform sample for cryo-EM analysis.

To stimulate the binding of MATCAP to microtubules and create a homogeneous sample for structural analysis, we sought a source of microtubules that is fully tyrosinated. To this end, a MATCAP and vasohibin-deficient cell line was created, which was used to extract fully tyrosinated microtubules. The extraction procedure was based on well-established protocols that use repeated cycles of polymerization and depolymerization of the microtubules to extract tubulin from brain tissue or cells^{18,27,28,29,30}, with only a single polymerization step and centrifugation over a glycerol cushion. Using MATCAP as an example, we then demonstrate how these microtubules can be used for cryo-EM studies. To prepare cryo-EM grids, a two-step application protocol at a low salt concentration is described. The methods in this paper describe the extraction of customizable microtubules at sufficient amounts and purity to perform cryo-EM analysis and provide a detailed protocol on how to use these microtubules to create protein-microtubule complexes on cryo-EM grids.

Protocol

NOTE: See the **Table of Materials** for details related to all the materials and equipment used in this protocol.

1. Cell culture

NOTE: All cell culture should be done in a sterile laminar flow hood.

1. To follow this protocol, first thaw a vial of frozen cells in a 37 °C water bath. Here, we use a genetically modified HCT116 cell line that lacks the three known

detyrosinating enzymes, VASH1, VASH2, and MATCAP, to create tyrosinated tubulin.

2. Prepare a Ø 10 cm plate containing 10 mL of the appropriate cell culture medium.

NOTE: In this protocol, DMEM (Dulbecco's modified Eagle medium) supplemented with 10% v/v FCS (fetal calf serum) and penicillin/streptomycin antibiotic (culture medium) was used for the genetically modified HCT116 cell line.

3. Count the cells, and seed $\sim 2.5 \times 10^6$ viable cells ($\sim 20\%$ confluence) in the prepared 10 cm plate. Shake the plate gently to evenly distribute the cells. Incubate the dish in a 37 °C cell-culture incubator gassed with 5% (v/v) CO₂ until the cells reach 80%-90% confluence.

NOTE: Typically, this takes 3 days for HCT116 cells, but the time could depend on the specific seeding density and cell line used.

4. Discard the cell culture medium using a pipette or vacuum aspirator and wash the dish 2 x 5 mL of PBS.

NOTE: Take care not to dispense the PBS too forcefully onto the cell monolayer as this could detach the cells from the plate.

5. Add 1-2 mL of trypsin, and incubate the cells in the incubator for 2-5 min to detach the cells.
6. Add 2 mL of the culture medium to the plate to quench the trypsin.
7. Split the cell suspension into three to five equal parts and reseed them to expand the cells in culture medium until 6-12 confluent 15 cm plates are obtained.

2. Harvesting

1. Wash the cells gently with 10 mL of PBS (1x) to remove any cell culture medium.

2. Detach the cells from the plates by incubating the cells for 5 min at room temperature with 3 mL of ice-cold PBS supplemented with 5 mM EDTA (sterile/filtered) and, subsequently, using a cell scraper.

3. Collect the cells in a 50 mL tube on ice, and spin down (10 min, 250 × g).

1. Note the volume of the harvested cells with the volumetric scale on the 50 mL tube.

NOTE: The expected volume can be anywhere between ~ 0.5 mL and 4 mL. PAUSE STEP: Flash-freeze the cell pellet in LN₂, and store at -20 °C until use. Note that the cell pellet can be stored only for a few weeks or months. If the pellet is kept longer, then it could result in a decreased yield or no microtubules at all.

3. Microtubule extraction

NOTE: Keep everything for steps 3.1-3.5 on ice; everything from step 3.6 onward should be kept warm (30-37 °C).

1. Prepare 10 mL of ice-cold lysis buffer containing 100 mM PIPES/KOH (pH 6.9), 2 mM EGTA/KOH, 1 mM MgCl₂, 1 mM PMSF, and one protease inhibitor tablet (mini).
2. Resuspend the harvested cell pellet in 1:1 v/v lysis buffer (if in doubt about the exact volume, take less lysis buffer rather than more).
3. Lyse the cells by sonication: 15 s on, 45 s off, amp 30, four cycles (determine the conditions experimentally, and change according to the sonicator).
 1. After sonication, collect a sample for SDS-PAGE analysis: 2 µL of lysate + 18 µL of water + 5 µL of 5x SDS sample buffer.

NOTE: Check under a standard light microscope if the cells have indeed fully lysed.

4. Pipette the lysed cells into a centrifugal tube. Spin for 1 h at $100,000 \times g$ at 4°C in an ultracentrifuge rotor to clear the lysate.

NOTE: Make sure all pockets in the rotor are dry and clean to ensure the correct balancing of the centrifuge.

5. Use a syringe to take the cleared lysate out. Take care to not disturb the pellet as well as the floating layer on top.

1. Collect a sample of the cleared lysate: $2\ \mu\text{L}$ of lysate + $18\ \mu\text{L}$ of water + $5\ \mu\text{L}$ of 5x SDS sample buffer.
2. Carefully rinse the pellet, and scoop up a little bit of the pellet by swirling a P10 pipette tip through the pellet; add $200\ \mu\text{L}$ of water and $50\ \mu\text{L}$ of SDS buffer.

6. Supplement the supernatant from the previous step with $1\ \text{mM}$ GTP and $20\ \mu\text{M}$ paclitaxel to polymerize the microtubules; for a volume of $1\ \text{mL}$, add $10\ \mu\text{L}$ of $2\ \text{mM}$ paclitaxel and $10\ \mu\text{L}$ of $100\ \text{mM}$ GTP.

CAUTION: Paclitaxel may cause skin irritation, serious eye damage, respiratory irritation, genetic defects, damage to an unborn child, and damage to organs. Prolonged or repeated exposure causes damage to organs. Do not breathe, spray, or dust the substance in any way. Wear rubber nitrile gloves to prevent skin contact.

7. Incubate the GTP/paclitaxel-supplemented supernatant for 30 min at 37°C to allow the microtubules to assemble.
8. During this incubation step, allow the rotor and the ultracentrifuge to warm up to 30°C .
9. Prepare the cushion buffer: Add $0.6\ \text{mL}$ of glycerol to $0.4\ \text{mL}$ of lysis buffer, and supplement the mixture with $20\ \mu\text{M}$ paclitaxel. Prewarm the cushion buffer to 37°C .

10. Add $800\ \mu\text{L}$ of cushion buffer to an ultracentrifuge tube. Pipette the GTP/paclitaxel-supplemented lysate carefully on top of the cushion buffer.

NOTE: Prevent the mixing of the cushion buffer and the lysate by pipetting very gently.

11. Spin for 30 min at $100,000 \times g$ at 30°C in an ultracentrifuge rotor. Mark the outward-facing edge of the centrifugation tube to easily recognize where the microtubule pellet should form.

12. Remove the cushion buffer carefully using a pipette, taking care not to disturb the microtubule pellet.

1. Collect a sample of the cushion buffer: $2\ \mu\text{L}$ + $18\ \mu\text{L}$ of water + $5\ \mu\text{L}$ of 5x SDS sample buffer.

13. Wash the pellet carefully 3x with warm lysis buffer to remove the glycerol. Gently dispense the warm buffer next to the pellet (not flushing the liquid directly over the pellet), rotate the tube a few times to remove as much glycerol as possible from the pellet and the walls of the tube, and then aspirate and repeat.

NOTE: If the glycerol is not washed off properly, the grid will melt very quickly under the electron illumination. This might be evidenced by high particle movement, creating blurry images.

14. Prepare resuspension buffer with the following ingredients: $100\ \text{mM}$ PIPES/KOH (pH 6.9), $2\ \text{mM}$ EGTA/KOH, and $1\ \text{mM}$ MgCl_2 , and warm the buffer to 37°C .

15. Resuspend the washed pellet gently with a cut tip in $\sim 50\ \mu\text{L}$ of prewarmed resuspension buffer, and keep the tube at 37°C .

1. Collect a sample of the resuspended pellet fraction: $2\ \mu\text{L}$ + $18\ \mu\text{L}$ of water + $5\ \mu\text{L}$ of 5x SDS sample buffer.

TIP: The cut tip prevents the breaking of the microtubules. Prepare a metal heating block to 37 °C, and keep this in a polystyrene box so that the sample tubes can be transported easily without cooling them down to room temperature.

4. Cryo-EM grid preparation

1. Prepare the plunge freezer device by installing the blotting paper. Warm the plunge freezer up to 30 °C, and set the humidification to 100%. Allow ~30 min to equilibrate the temperature and humidity.
2. Prepare the settings of the plunge freezer to two applications, and run through the whole program once to be sure the settings are set properly. Ensure that the first application has a force of 10, 2 s blot time, and 0 s wait time and that the second application has a force of 10, 6.5 s blot time, and 10 s wait time.
3. Glow-discharge the cryo-EM grids at 30 mA for 60 s.
4. Cool the polystyrene container assembly down with LN₂, and prepare liquid ethane in a metal cup by condensing ethane gas into a cold metal cup.
5. Prepare a dilution buffer with the following components: 100 mM PIPES/KOH (pH 6.9), 2 mM EGTA/KOH, and 1 mM MgCl₂, and warm it to 37 °C.
6. Dilute the microtubule-interacting protein 1:1 v/v with dilution buffer just before applying it to the grids to ensure the salt concentration is lowered (we used a final salt concentration of 50 mM NaCl). Keep the mixture at 37 °C.
7. Grab a glow-discharged grid with plunge-tweezers and click them into the plunge freezer.
8. Position the polystyrene container with liquid ethane in the plunge freezer, and run through the prepared

program: first apply 3.5 µL of microtubule solution to the grid, let the plunge freezer blot the grid, then immediately apply 3.5 µL of freshly diluted protein, and lastly, let the plunger blot and plunge-freeze the grid in liquid ethane.

9. Transfer the grids into a grid storage box, and store them in an LN₂ dewar until imaging.

Representative Results

We investigated the tubulin detyrosinase MATCAP bound to tyrosinated microtubules by cryo-EM. To do so, we extracted fully tyrosinated microtubules from a genetically modified HCT116 cell line lacking all three known detyrosinating enzymes, VASH1/2 and MATCAP. We used 6-12 confluent 15 cm dishes to extract the microtubules from approximately 0.5-4 mL of cell pellet (**Figure 1**). After the second centrifugation step (step 3.11), this yields a visible but small and transparent pellet (**Figure 1I**). The microtubule yield is typically ~75 µg. If the pellet is not visible, this might indicate a problem in one of the previous steps, such as an incorrect microtubule polymerization temperature, problems with the quality of the used GTP or paclitaxel, or the addition of too much lysis buffer, resulting in a tubulin concentration that is too low for polymerization. To assess the quality and concentration of the extracted microtubules, we analyzed samples on a Coomassie-stained SDS gel (**Figure 2A**). These analyses indicated that the extracted microtubules were relatively pure. The interpolated microtubule concentration derived from BSA quantification was ~1.4 mg/mL. This agrees well with the number measured with a spectrophotometer (**Figure 2B,C**).

The freshly extracted microtubules can directly be used to make samples for cryo-EM. The microtubules should look intact and abundant on the micrographs. For further cryo-EM analysis, it is key to have a low microtubule density per

micrograph to avoid the microtubules crossing over each other (**Figure 3A**). Broken microtubules or those that are not visible might indicate that the microtubules depolymerized (e.g., due to a low temperature or GTP hydrolysis) or that the blotting and plunge freezing parameters were not set correctly. The background around the microtubules is dense, presumably with unpolymerized tubulin.

The molecular weight of MATCAP is 53 kDa, and it has a globular catalytic domain just below the size of a tubulin monomer. The decoration of MATCAP on the microtubule could, therefore, be detected visually. Microtubules that did not bind MATCAP showed "smooth" edges, whereas microtubules that bound MATCAP had "rough" edges, characterized by electron-dense dots on

the microtubule surface (**Figure 3B**). MATCAP-bound and MATCAP-unbound microtubules could also be distinguished in the calculated 2D classes, although due to shape and size, this might differ for other microtubule-interacting proteins (**Figure 3C**). To confirm that the density indeed belongs to the protein of interest, one can take advantage of experimentally determined or predicted structures. We also suggest making a control grid that contains microtubules only for comparison. This indicates whether the microtubules were polymerized and extracted intact at a sufficiently high concentration and that the plunge freezing process was executed correctly. We noticed that the microtubule abundance decreased in grids with a second MATCAP application.

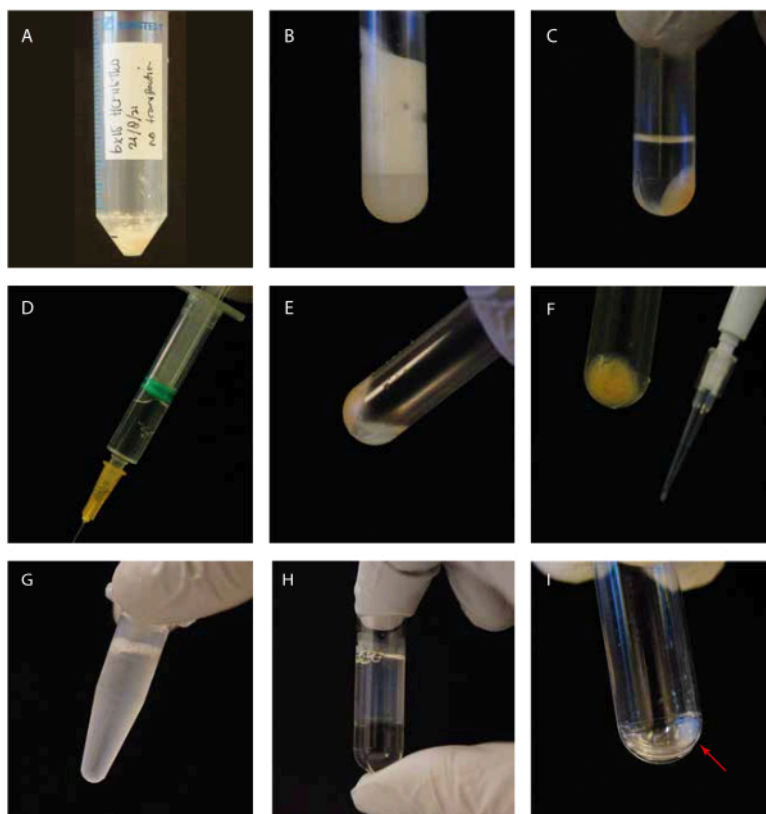


Figure 1: Visual guidance of the experimental steps. (A) Cell pellet before lysis; (B) sonicated cells in an ultracentrifuge tube before centrifugation; (C) sonicated cells in an ultracentrifuge tube after centrifugation; (D) syringe with the cleared supernatant; (E) residual pellet after supernatant removal, including a "white floating layer"; (F) P10 tip with a cell debris pellet for the SDS Coomassie gel; (G) GTP/paclitaxel-supplemented supernatant before incubation; (H) GTP/paclitaxel-incubated supernatant on top of a glycerol cushion in an ultracentrifuge tube; (I) clean microtubule pellet after the second centrifugation step. [Please click here to view a larger version of this figure.](#)

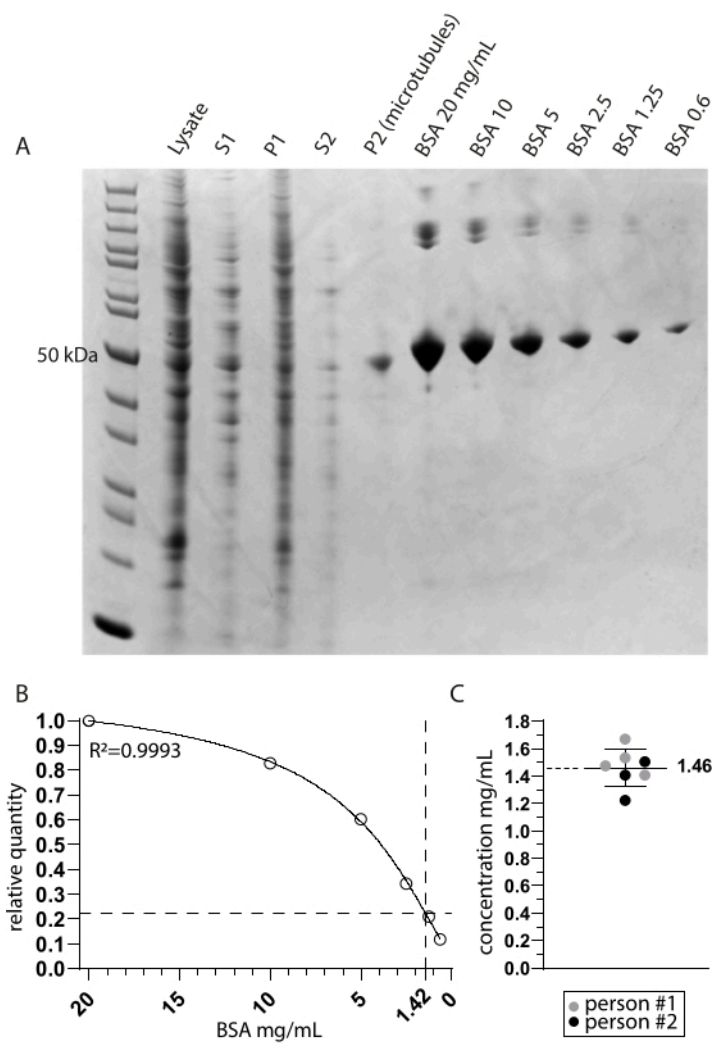


Figure 2: Microtubule purity and concentration determination. (A) Coomassie-stained SDS page gel showing the samples taken during the extraction protocol and a BSA concentration comparison. S1 and P1 correspond to the supernatant and pellet after the first centrifugation step, respectively. S2 and P2 similarly correspond to the second centrifugation step. (B) A non-linear regression line of the relative BSA quantities derived from A. The interpolation of the microtubule band around 50 kDa in the P2 (microtubules) lane indicates a final concentration of 1.42 mg/mL. (C) The spectrophotometric analysis of the resuspended microtubules (P2) measured by two people and corrected for the combined extinction coefficient of TUBA1A and TUBB3 (0.971) indicates a mean and standard deviation concentration of 1.46 mg/mL \pm 0.14 mg/mL. [Please click here to view a larger version of this figure.](#)

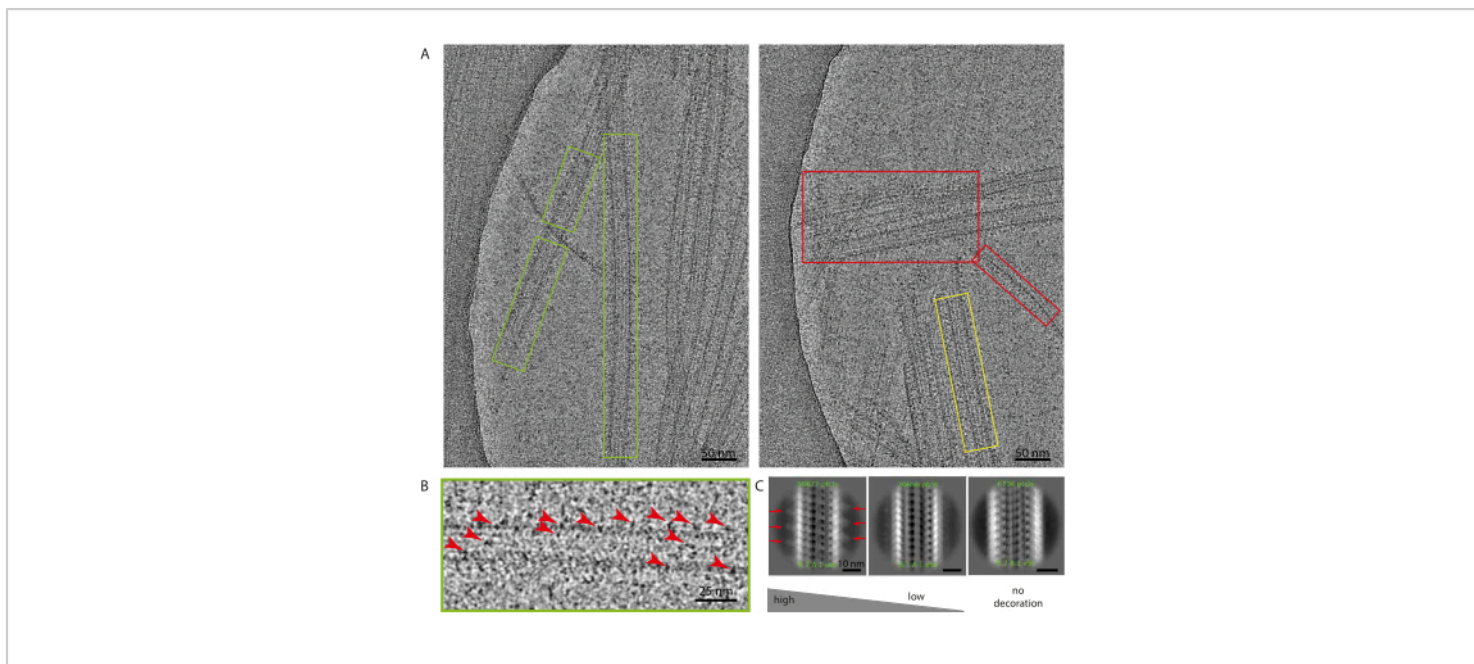


Figure 3: Example micrographs. (A) Example micrographs showcasing microtubules bound to MATCAP. The microtubules indicated by a green box are intact, decorated, and can be used for the cryo-EM analysis. The microtubule indicated by the orange box is an intact and decorated microtubule but is positioned close to the microtubules left of it; therefore, it is less suitable to include in the cryo-EM analysis. The microtubules in the red box are crossing over and broken. These should be excluded from the cryo-EM analysis. (B) A zoomed-in view of the green encircled microtubule of the left panel. The red arrowheads indicate the black dots that only appeared on the microtubules in the micrographs that had an application of MATCAP and, thus, likely correspond to MATCAP bound to the microtubule. (C) Example 2D classes of microtubule particles picked from A that showed high and low decoration and a 2D class from a different dataset for which we observed no decoration by MATCAP (right-most panel). Scale bars = (A) 50 nm, (B) 25 nm, (C) 10 nm. [Please click here to view a larger version of this figure.](#)

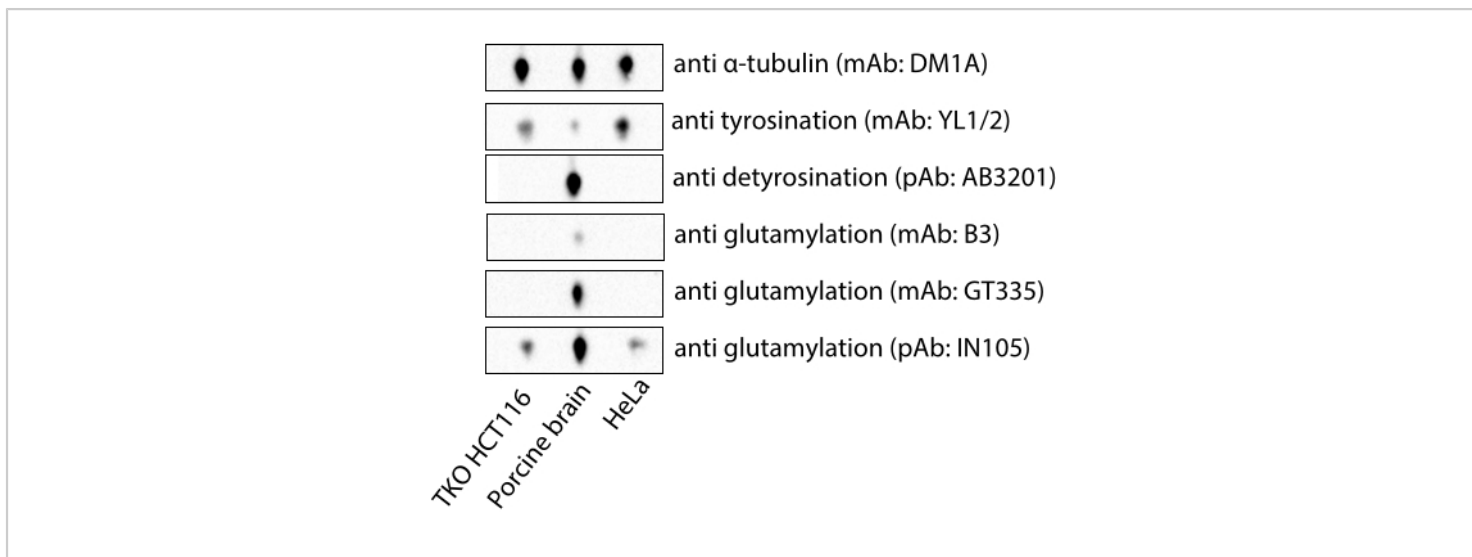


Figure 4: Immunoblot analysis of microtubules derived from MATCAP-deficient and VASH1/2-deficient triple knockout (TKO) HCT116 cells, commercial porcine brain, and HeLa tubulin. Abbreviations: TKO = triple knockout; mAb = monoclonal antibody; pAb = polyclonal antibody. [Please click here to view a larger version of this figure.](#)

Discussion

This method describes how to rapidly extract endogenous tubulin from cell lines and subsequently decorate those microtubules on cryo-EM grids. Microtubules are temperature-sensitive. They depolymerize in a cold environment and polymerize in a warm environment³¹. It is, therefore, critical to execute the sonication and clearance spin (steps 1.1-1.5) at 4 °C to solubilize the tubulin. If any factors were stabilizing the microtubules so well that they would not depolymerize in this step, these microtubules and the stabilizing factors would be discarded in the pellet after the initial clearance spin. After (re)polymerizing the microtubules, it is important to keep the solution containing the polymerized microtubules warm at all times. We extracted the microtubules from HCT116 cells, which are deficient in the VASH1, VASH2, and MATCAP proteins. Other cell lines, as well as tissues, can be used to extract microtubules²⁹, although the contaminants, tubulin isotypes, and yield could

be very different from what is described here. Overexpressing plasmids that contain modifying enzymes can also be used to introduce specific tubulin modifications.

Other protocols^{18,27,28,29,30} use multiple cycles of polymerization and depolymerization of the microtubules to obtain microtubules void of other interacting proteins. Here, we have simplified these protocols and only polymerize the microtubules once. It is possible that because of this single polymerization, these microtubules may co-sediment with other microtubule-interacting proteins. However, we have found that this protocol gives sufficiently pure microtubules for cryo-EM purposes. If a purer sample is needed for specific assays, additional cycles of polymerization and depolymerization could yield a purer sample, though this might be at the expense of the microtubule yield. In this protocol, we used paclitaxel to polymerize the microtubules. However, paclitaxel could bias the microtubule lattice toward a certain twist and rise, which could interfere with

the microtubule affinity of the protein of interest. Other microtubule-stabilizing reagents could be used if paclitaxel is unsuitable; examples of these reagents are non-taxane molecules such as peloruside or non-hydrolyzable GTP variants such as GMPCPP^{17,32}.

To structurally investigate proteins that bind to microtubules on cryo-EM grids, one needs to bind a sufficient amount of the protein of interest to the microtubules. A commonly occurring problem is that protein complexes that are stable in solution fall apart on the grid. For forming the protein complex on the grid, it was crucial to first layer the microtubules and then apply the microtubule-binding protein with a low salt concentration to the microtubule-coated grid, thus assembling the protein complex directly on the grid. Others have similarly reported a low-salt^{33,34} protocol and a two-step application^{34,35,36} protocol for successful microtubule decoration. It is likely that a lower salt concentration biases the protein complex toward a more stable interaction due to the decreased electrostatic charges. However, due to the low salt concentration, the protein of interest is at risk for precipitating. Therefore, it is highly recommended to keep the protein at or around physiologically relevant salt concentrations until shortly before vitrifying the grids. This two-step application protocol likely prevents the protein complex from falling apart during the blotting or plunge-freezing steps. In this protocol, we used the Vitrobot. However, faster vitrification methods (VitroJet) or the use of blot-free grids (Puffalot) or devices that have both properties (chameleon) could potentially overcome the two-step application, but these are currently not widely available for testing.

The final resolution of the reconstructed cryo-EM density can be affected by a number of factors, including the movement of the microtubule-binding protein relative to the

microtubule and the level of decoration that can be achieved. Higher microtubule decoration is likely beneficial to the final resolution obtained in the 3D density reconstruction. This can be limited by a few factors, such as the highest protein concentration that is obtained during the purification of the microtubule-binding protein, the lowest salt concentration that the microtubule-interacting protein can withstand without aggregating, and the binding mode of the microtubule-interacting protein (e.g., the protein could span more than one tubulin dimer, thus hindering a 1:1 binding ratio). Although the resolution of the cryo-EM reconstruction might be compromised by sparsely decorated microtubules, computational analysis can circumvent a lot of problems, as exemplified by a recently reported microtubule-protein complex structure that was extremely sparsely decorated⁸.

The protocol we describe here presents a quick, low-cost method to obtain microtubules suitable for cryo-EM purposes. In contrast to commercially available porcine brain tubulin, the microtubules derived from MATCAP-deficient and vasohibin-deficient HCT116 cells are fully tyrosinated (**Figure 4**). Commercial HeLa tubulin, an expensive reagent, in principle, is relatively uniformly tyrosinated and contains little other modifications⁴ such as glutamylation, but batches might vary, and modification could only be achieved *in vitro*. An advantage of extracting microtubules from custom-made cell lines is the flexibility one has to overexpress or delete tubulin-modifying enzymes, such as tubulin detyrosinases, to create a more homogeneous pool of microtubules. This can benefit the decoration and uniformity of the cryo-EM sample and will ultimately benefit the ease and quality of the cryo-EM density maps and molecular structures derived from this sample.

Disclosures

The authors have no conflicts of interest to disclose.

Acknowledgments

We thank all the members of the Sixma, Brummelkamp, and Perrakis groups for their fruitful scientific discussions and for providing a pleasant working environment, and specifically, we thank Jan Sakoltchik ("person 2") for helping to determine the protein concentration depicted in **Figure 3C**. We would also like to thank the NKI cryo-EM facility and the Netherlands Centre for Electron Nanoscopy (NeCEN) at Leiden University for their support. This work was supported by NWO Vici grant 016.Vici.170.033 awarded to T.R.B.. A.P. and T.R.B. are Oncode investigators and receive funding from NWO ENW (OCENW.M20.324). L.L. received funding from the Austrian Science Fund (FWF JB4448-B). This research was supported by an institutional grant of the Dutch Cancer Society and of the Dutch Ministry of Health, Welfare and Sport.

References

1. Janke, C., Magiera, M. M. The tubulin code and its role in controlling microtubule properties and functions. *Nature Reviews Molecular Cell Biology*. **21** (6), 307-326 (2020).
2. Peris, L. et al. Motor-dependent microtubule disassembly driven by tubulin tyrosination. *Journal of Cell Biology*. **185** (7), 1159-1166 (2009).
3. McKenney, R. J., Huynh, W., Tanenbaum, M. E., Bhabha, G., Vale, R. D. Activation of cytoplasmic dynein motility by dynactin-cargo adapter complexes. *Science*. **345** (6194), 337-341 (2014).
4. Barisic, M. et al. Microtubule detyrosination guides chromosomes during mitosis. *Science*. **348** (6236), 799-803 (2015).
5. Sirajuddin, M., Rice, L. M., Vale, R. D. Regulation of microtubule motors by tubulin isotypes and post-translational modifications. *Nature Cell Biology*. **16** (4), 335-344 (2014).
6. Nogales, E., Kellogg, E. H. Challenges and opportunities in the high-resolution cryo-EM visualization of microtubules and their binding partners. *Current Opinion in Structural Biology*. **46**, 65-70 (2017).
7. Manka, S. W., Moores, C. A. Microtubule structure by cryo-EM: Snapshots of dynamic instability. *Essays in Biochemistry*. **62** (6), 737-751 (2018).
8. Chaaban, S., Carter, A. P. Structure of dynein-dynactin on microtubules shows tandem adaptor binding. *Nature*. **610** (7930), 212-216 (2022).
9. Lacey, S. E., He, S., Scheres, S. H., Carter, A. P. Cryo-EM of dynein microtubule-binding domains shows how an axonemal dynein distorts the microtubule. *eLife*. **8**, e47145 (2019).
10. Walton, T., Wu, H., Brown, A. Structure of a microtubule-bound axonemal dynein. *Nature Communications*. **12**, 477 (2021).
11. Sindelar, C. V., Downing, K. H. An atomic-level mechanism for activation of the kinesin molecular motors. *Proceedings of the National Academy of Sciences of the United States of America*. **107** (9), 4111-4116 (2010).
12. Zhang, R., Alushin, G. M., Brown, A., Nogales, E. Mechanistic origin of microtubule dynamic instability and

- its modulation by EB proteins. *Cell*. **162** (4), 849-859 (2015).
13. Maurer, S. P., Fourniol, F. J., Bohner, G., Moores, C. A., Surrey, T. EBs Recognize a nucleotide-dependent structural cap at growing microtubule ends. *Cell*. **149** (2), 371-382 (2012).
 14. Benoit, M. P. M. H., Asenjo, A. B., Sosa, H. Cryo-EM reveals the structural basis of microtubule depolymerization by kinesin-13s. *Nature Communications*. **9**, 1662 (2018).
 15. Kellogg, E. H. et al. Near-atomic model of microtubule-tau interactions. *Science*. **360** (6394), 1242-1246 (2018).
 16. Brotzakis, Z. F. et al. A structural ensemble of a Tau-microtubule complex reveals regulatory Tau phosphorylation and acetylation mechanisms. *ACS Central Science*. **7** (12), 1986-1995 (2021).
 17. Kellogg, E. H. et al. Insights into the distinct mechanisms of action of taxane and non-taxane microtubule stabilizers from cryo-EM structures. *Journal of Molecular Biology*. **429** (5), 633-646 (2017).
 18. Vallee, R. B. Reversible assembly purification of microtubules without assembly-promoting agents and further purification of tubulin, microtubule-associated proteins, and MAP fragments. *Methods in Enzymology*. **134**, 89-104 (1986).
 19. Wloga, D., Joachimiak, E., Louka, P., Gaertig, J. Posttranslational modifications of tubulin and cilia. *Cold Spring Harbor Perspectives in Biology*. **9** (6), a028159 (2017).
 20. Nieuwenhuis, J., Brummelkamp, T. R. The tubulin detyrosination cycle: Function and enzymes. *Trends in Cell Biology*. **29** (1), 80-92 (2019).
 21. Nieuwenhuis, J. et al. Vasohibins encode tubulin detyrosinating activity. *Science*. **358** (6369), 1453-1456 (2017).
 22. Aillaud, C. et al. Vasohibins/SVBP are tubulin carboxypeptidases (TCPs) that regulate neuron differentiation. *Science*. **358** (6369), 1448-1453 (2017).
 23. Landskron, L. et al. Posttranslational modification of microtubules by the MATCAP detyrosinase. *Science*. **376** (6595), eabn6020 (2022).
 24. Erck, C. et al. A vital role of tubulin-tyrosine-ligase for neuronal organization. *Proceedings of the National Academy of Sciences of the United States of America*. **102** (22), 7853-7858 (2005).
 25. Pagnamenta, A. T. et al. Defective tubulin detyrosination causes structural brain abnormalities with cognitive deficiency in humans and mice. *Human Molecular Genetics*. **28** (20), 3391-3405 (2019).
 26. Peris, L. et al. Tubulin tyrosination regulates synaptic function and is disrupted in Alzheimer's disease. *Brain*. **145** (7), 2486-2506 (2022).
 27. Souphron, J. et al. Purification of tubulin with controlled post-translational modifications by polymerization-depolymerization cycles. *Nature Protocols*. **14** (5), 1634-1660 (2019).
 28. Gell, C. et al. Purification of tubulin from porcine brain. *Methods in Molecular Biology*. **777**, 15-28 (2011).
 29. Bodakuntla, S., Jijumon, A. S., Janke, C., Magiera, M. M. Purification of tubulin with controlled posttranslational modifications and isotypes from limited sources by polymerization-depolymerization cycles. *Journal of Visualized Experiments*. (165), e61826 (2020).

30. Castoldi, M., Popov, A. V. Purification of brain tubulin through two cycles of polymerization-depolymerization in a high-molarity buffer. *Protein Expression and Purification*. **32** (1), 83-88 (2003).
31. Li, G., Moore, J. K. Microtubule dynamics at low temperature: evidence that tubulin recycling limits assembly. *Molecular Biology of the Cell*. **31** (11), 1154-1166 (2020).
32. Hyman, A. A., Salser, S., Drechsel, D. N., Unwin, N., Mitchison, T. J. Role of GTP hydrolysis in microtubule dynamics: information from a slowly hydrolyzable analogue, GMPCPP. *Molecular Biology of the Cell*. **3** (10), 1155-1167 (1992).
33. Sindelar, C. V., Downing, K. H. The beginning of kinesin's force-generating cycle visualized at 9-Å resolution. *Journal of Cell Biology*. **177** (3), 377-385 (2007).
34. Kellogg, E. H. et al. Near-atomic cryo-EM structure of PRC1 bound to the microtubule. *Proceedings of the National Academy of Sciences of the United States of America*. **113** (34), 9430-9439 (2016).
35. Maurer, S. P., Bieling, P., Cope, J., Hoenger, A., Surrey, T. GTPγS microtubules mimic the growing microtubule end structure recognized by end-binding proteins (EBs). *Proceedings of the National Academy of Sciences of the United States of America*. **108** (10), 3988-3993 (2011).
36. Manka, S. W., Moores, C. A. Pseudo-repeats in doublecortin make distinct mechanistic contributions to microtubule regulation. *EMBO Reports*. **21** (12), e51534 (2020).